

Biophysical Journal, Volume 113

Supplemental Information

**Asymmetric Phosphatidylethanolamine Distribution Controls Fusion
Pore Lifetime and Probability**

**Alex J.B. Kreuzberger, Volker Kiessling, Binyong Liang, Sung-Tae Yang, J. David
Castle, and Lukas K. Tamm**

Materials and Methods

Materials

The following materials were purchased and used without further purification: porcine brain L- α -phosphatidylcholine (bPC), porcine brain L- α -phosphatidylethanolamine (bPE), porcine brain L- α -phosphatidylserine (bPS), bovine liver L- α -phosphatidylinositol (PI), phosphatidylinositol 4,5-bisphosphate (PI4,5P₂), 1,2-dioleoyl-*sn*-glycero-3-phosphoethanolamine-N-(lissamine rhodamine B sulfonyl) (Rh-DOPE), and 1,2-dioleoyl-*sn*-glycero-3-phosphoethanolamine-N-(7-nitro-2-1,3-benzoxadiazol-4-yl) (NBD-DOPE) were from Avanti Polar Lipids (Alabaster, AL). 1,2-dimyristoyl-*sn*-glycero-3--phosphoethanolamine-PEG3400-triethoxysilane (DPS) was from Shearwater Polymers (Huntsville, AL). Cholesterol, sodium cholate, 2,2',2'',2'''-(ethane-1,2-diyldinitrilo)tetraacetic acid (EDTA), calcium (Ca²⁺), OptiPrep density gradient medium, sucrose, 3-(N-morpholino)propanesulfonic acid (MOPS), L-glutamic acid potassium salt monohydrate, potassium acetate, and glycerol were from Sigma (St. Louis, MO); 3-[(3-cholamidopropyl)dimethylammonio]-1-propanesulfonate (CHAPS) and dodecylphosphocholine (DPC) were from Anatrace (Maumee, OH); 2-[4-(2-hydroxyethyl)piperazin-1-yl]ethanesulfonic acid (HEPES) was from Research Products International (Mount Prospect, IL); chloroform, ethanol, Contrad detergent, all inorganic acids, bases, and hydrogen peroxide were from Fisher Scientific (Fair Lawn, NJ). Water was purified first with deionizing and organic-free 3 filters (Virginia Water Systems, Richmond, VA) and then with a NANOpure system from Barnstead (Dubuque, IA) to achieve a resistivity of 18.2 M Ω /cm.

Protein purification

Syntaxin-1a (constructs of residues 183-288) and wild-type SNAP-25A from *Rattus norvegicus* were expressed in *Escherichia coli* strain BL21(DE3) cells under the control of the T7 promoter in the pET28a expression vector and purified as described previously (21-24). Briefly, all proteins were purified using the Ni-NTA affinity chromatography. After the removal of N-terminal His-tags by thrombin cleavage, proteins were further purified by subsequent ion-exchange or size-exclusion chromatography when necessary. Wild-type SNAP-25 was quadruply dodecylated through disulfide bonding of dodecyl methanethiosulfonate (Toronto Research Company, Toronto, Ontario) to its four native cysteines (24). All SNAP-25 used in this work

refers to this lipid-anchored form of SNAP-25A. Purities of all proteins were verified by SDS-PAGE.

Reconstitution of SNAREs into proteoliposomes

Proteoliposomes with lipid composition of 25:25:15:30:4:1 bPC:bPE:bPS:Chol:PI: PI4,5P₂ for PE in the distal leaflet or 50:15:30:4:1 bPC:bPS:Chol:PI: PI4,5P₂ for no PE in the proximal leaflet were prepared. All t-SNARE proteins were reconstituted using sodium cholate as previously described (25, 26). The desired lipids were mixed and organic solvents were evaporated under a stream of N₂ gas followed by vacuum desiccation for at least 1 hour. The dried lipid films were dissolved in 181 μ L of 25 mM sodium cholate in buffer (20 mM HEPES, 150 mM KCl, pH 7.4) followed by the addition of an appropriate volume of syntaxin-1a and SNAP-25A in their respective detergents to reach a final lipid to protein ratio of 3000 for each protein. After 1 hour of equilibration at room temperature, the mixture was diluted below the critical micellar concentration by adding more buffer to the desired final volume of 550 μ L. The sample was then dialyzed overnight against 1 L of buffer with 1 buffer change after ~4 hours.

Preparation of planar supported bilayers containing SNARE acceptor complexes

Planar supported bilayers with reconstituted plasma membrane SNAREs were prepared by the Langmuir-Blodgett/vesicle fusion technique as described in previous studies (15, 26). Quartz slides were cleaned by dipping in 3:1 sulfuric acid:hydrogen peroxide for 15 minutes using a Teflon holder. Slides were then rinsed thoroughly in water. The first leaflet of the bilayer was prepared by Langmuir-Blodgett transfer directly onto the quartz slide using a Nima 611 Langmuir-Blodgett trough (Nima, Coventry, UK) by applying the lipid mixture of 70:30:3 bPC:Chol:DPS for no PE in the proximal leaflet or 45:25:30:3 bPC:bPE:Chol:DPS for PE in the proximal leaflet from a chloroform solution. After allowing the solvent to evaporate for 10 minutes, the monolayer was compressed at a rate of 10 cm²/minute to reach a surface pressure of 31 mN/m. After equilibration for 5 to 10 minutes, a clean quartz slide was rapidly (200 mm/minute) dipped into the trough and slowly (5 mm/minute) withdrawn, while a computer maintained a constant surface pressure and monitored the transfer of lipids with head groups down onto the hydrophilic substrate. Proteoliposomes reconstituted with 1:1 syntaxin-1a (residues 183-288):SNAP-25 at a lipid/protein ratio of 3000 were incubated with the Langmuir-

Blodgett monolayer to form the outer leaflet of the planar supported bilayer. A concentration of 77 μM total lipid in 1.3 mL total volume was used and the lipid composition of the outer leaflet was as indicated in the text. After incubation of the proteoliposomes for 2 hours the excess proteoliposomes were removed by perfusion with 10 mL of buffer (120 mM potassium glutamate, 20 mM potassium acetate, 20 mM HEPES, pH 7.4). The reconstitution efficiencies and orientation of syntaxin-1a under the four membrane preparations were almost identical. This was measured using site directed fluorescence labeling and Co^{2+} quenching as previously described (22) and illustrated in Supplemental Figure S2.

Cell culture

As previously described (14), pheochromocytoma cells (PC12) were cultured on 10 cm plastic cell culture plates at 37°C in 10% CO_2 in Dulbecco's Modified Eagle Medium (DMEM) High Glucose 1 X Gibco supplemented with 10% horse serum (Cellgro), 10% calf serum (Fe^+) (Hyclone), and 1% penicillin/streptomycin mix. Medium was changed every 2-3 days and cells were passed after reaching 90% confluency by incubating 5 min in HBSS and replating in fresh medium. Cells were transfected with a plasmid carrying NPY-mRuby (14) by electroporation using an Electro Square Porator ECM 830 (BTX). After harvesting and sedimentation, cells were suspended in a small volume of sterile cytomix electroporation buffer (27) (120 mM KCl, 10 mM KH_2PO_4 , 0.15 mM CaCl_2 , 2 mM EGTA, 25 mM HEPES-KOH, 5 mM MgCl_2 , 2 mM ATP, and 5 mM glutathione, pH 7.6) and then counted and diluted to $\sim 14 \times 10^6$ cells/mL. 700 μL of cell suspension ($\sim 10 \times 10^6$ cells) and 30 μg of DNA were placed in an electroporation cuvette with 4 mm gap and two 255V, 8 ms electroporation pulses were applied. Cells were then transferred to a 10 cm cell culture dish with 10 mL of normal growth medium. NPY-mRuby transfected cells were cultured under normal conditions for 3 days after transfection and then used for fractionation.

DCV purification

As previously described (14), DCVs were purified using iso-osmotic media as follows. PC12 cells (15-30 10-cm plates depending on experiments) were scraped into PBS, pelleted by centrifugation, resuspended, and washed once in homogenization medium (0.26 M sucrose, 5 mM MOPS, and 0.2 mM EDTA). Following resuspension in 3 mL homogenization medium

containing protease inhibitor (Roche Diagnostics), the cells were cracked open using a ball bearing homogenizer with a 0.2507-inch bore and 0.2496-inch diameter ball. The homogenate was then spun at 4000 rpm (1000 x g) for 10 min at 4°C in a fixed-angle microcentrifuge to pellet nuclei and larger debris. The postnuclear supernatant (PNS) was collected and spun at 11,000 rpm (8000 x g), 15 min at 4°C to pellet mitochondria. The postmitochondrial supernatant (PMS) was then collected, adjusted to 5 mM EDTA, and incubated for 10 min on ice. A working solution of 50% Optiprep (iodixanol) (5 vol 60% Optiprep: 1 vol 0.26 M sucrose, 30 mM MOPS, 1 mM EDTA) and homogenization medium were mixed to prepare solutions for discontinuous gradients in Beckman SW55 tubes: 0.5 mL of 30% iodixanol on the bottom and 3.8 mL of 14.5% iodixanol, above which 1.2 ml EDTA-adjusted PMS was layered. Samples were spun at 45,000 rpm (190,000 x g_{av}) for 5 hours. A clear white band at the interface between the 30% and 14.5% iodixanol regions was collected as the DCV sample. The DCV sample was then extensively dialyzed in a cassette with 10,000 kD molecular weight cutoff (24-48 h, 3 x 5L) into the fusion assay buffer (120 mM potassium glutamate, 20 mM potassium acetate, 20 mM HEPES, pH 7.4).

Total internal reflection fluorescence (TIRF) microscopy

Experiments examining single-vesicle docking and fusion events were performed on a Zeiss Axiovert 35 fluorescence microscope (Carl Zeiss, Thornwood, NY), equipped with a 63x water immersion objective (Zeiss; N.A. = 0.95) and a prism-based TIRF illumination. The light source was an OBIS 532 LS laser from Coherent Inc. (Santa Clara, CA). Fluorescence was observed through a 610 nm band pass filter (D610/60; Chroma, Battleboro, VT) by an electron multiplying CCD (DU-860E; Andor Technologies). The prism-quartz interface was lubricated with glycerol to allow easy translocation of the sample cell on the microscope stage. The beam was totally internally reflected at an angle of 72° from the surface normal, resulting in an evanescent wave that decays exponentially with a characteristic penetration depth of ~100 nm. An elliptical area of 250 x 65 μm was illuminated. The laser intensity, shutter, and camera were controlled by a homemade program written in LabVIEW (National Instruments, Austin, TX).

Single DCV fusion assay

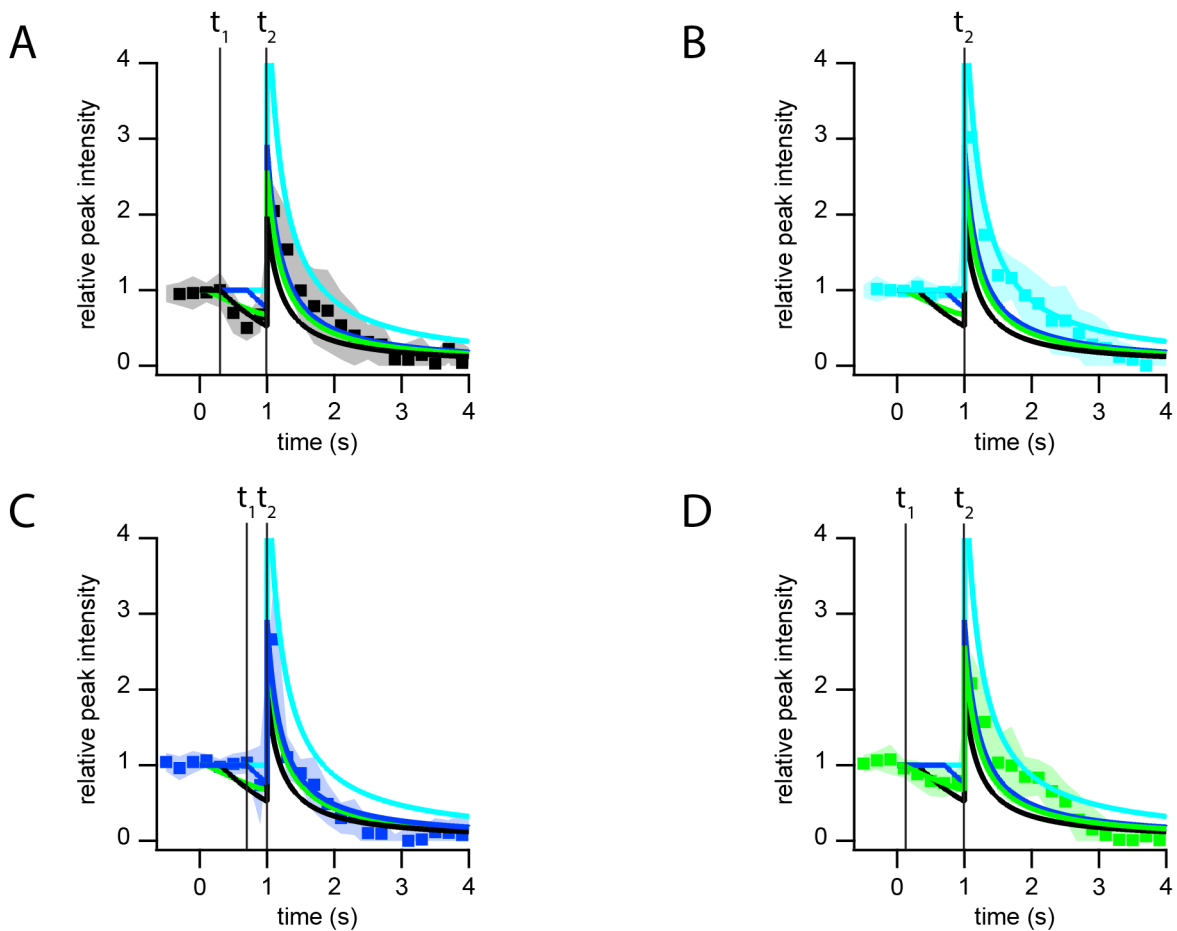
Acceptor t-SNARE protein-containing planar supported bilayers were washed with fusion buffer containing EDTA. They were then perfused with DCVs (50-100 μ L depending on preparation) diluted into 2 mL of fusion buffer (120 mM potassium glutamate, 20 mM potassium acetate, 20 mM HEPES, 100 μ M EDTA, pH 7.4). After injection of the DCV sample, the microscope was focused within no more than 30 seconds and then 5000 images were taken with 200-ms exposure times and spooled directly to the hard drive. One spooling set was taken for each bilayer.

Single-vesicle fusion data were analyzed using a homemade program written in LabView (National Instruments). Stacks of images were filtered by a moving average filter. The maximum intensity for each pixel over the whole stack was projected on a single image. Vesicles were located in this image by a single-particle detection algorithm described in Kiessling et al. (28). The peak (central pixel) and mean fluorescence intensities of a 5 pixel x 5 pixel area around each identified center of mass were plotted as a function of time for all particles in the image series. The exact time points of docking and fusion were determined from the central pixel similar to previous work (25). Cumulative distributions were determined from the time of docking to the time of fusion for individual fusion events and the fusion efficiency was determined from the number of vesicles that underwent fusion compared with the total number of vesicles that docked within 15 seconds of DCV docking.

Supplemental Results

Two-step Mathematical Fusion/Diffusion Model to Simulate Single DCV Fluorescence Intensity Traces

The fluorescence signal originating from the DCVs during fusion follows a characteristic line shape (Figure 1, Supplemental Figure 1). In the following paragraphs we reiterate a previously published description of a simple 2-step fusion/diffusion model that reproduces the basic features of the signal (14).



Supplemental Figure S1: Averaged peak fluorescence during single DCV fusion events to supported membranes with four different trans-bilayer PE distributions: A) PE in the distal leaflet (black). B) PE in the proximal leaflet (cyan). C) PE in both leaflets (blue). D) without PE (green). The data are normalized to the intensity during docking, i.e. before fusion starts. For comparison, we combined the best simulated curves of all conditions with each data set.

At each time the fluorescence originating from the fluorophore mRuby is determined by the sum of the fluorophore fraction located in the lumen of the DCV at a concentration C_{DCV} and the fraction in the small cleft between supported membrane and substrate at concentration C_{CLEFT} :

$$I = I_{DCV}(C_{DCV}(t, x, y), \lambda) + I_{CLEFT}(C_{CLEFT}(t, x, y, D), \lambda) \quad (1)$$

The model starts with a DCV of diameter $d_{DCV} = 200$ nm (28) docked at the supported lipid bilayer at distance $z_0 = 8$ nm (30) from the substrate and at $x, y = 0$. For the observed intensities, we take into account the 2D point spread function at $\lambda = 600$ nm and the decay of the evanescent wave with a characteristic penetration depth of $d_p = 100$ nm:

$$I_0 = I_{DCV}(t < t_1) = PSF(\lambda) * \int_{z_0}^{z_0 + d_{DCV}} C_{DCV}(x, y, z) e^{\frac{-z}{d_p}} dz \quad (2)$$

At time t_1 a fusion pore opens and content from the DCV gets released through the supported membrane into the cleft with a characteristic rate k_r at $x, y = 0$:

$$r(t - t_1) = e^{-\frac{(t-t_1)}{k_r}} \quad (3)$$

It is important to note that the characteristic rate might be limited by the release from the DCV's luminal structure or the diffusion through the fusion pore. Fluorescent content in the cleft is located at an average distance $z_{CLEFT} = 2$ nm (29) and spreads laterally in the x, y plane by free diffusion characterized by a diffusion coefficient D_1 .

$$dC_{CLEFT}(t_1 < t < t_2) = [dr + D_1 \Delta C_{CLEFT}] dt \quad (4)$$

$$I_{CLEFT}(t_1 < t < t_2) = PSF(\lambda) * C_{CLEFT}(x, y, z, t) e^{\frac{-z_{CLEFT}}{d_p}} \quad (5)$$

During the life time of the fusion pore ($t_1 < t < t_2$) the shape of the DCV stays intact and content gets released from membrane proximal areas first (Figure 1A). A simpler model in which the distribution of content inside the DCV stays homogenous did not fit the data sufficiently. The fluorescence intensity originating from the DCV during this phase becomes:

$$I_{DCV}(t_1 < t < t_2) = PSF(\lambda) * \int_{z_1(t)}^{z_0 + d_{DCV}} C_{DCV}(x, y, z) e^{\frac{-z}{d_p}} dz \quad (6)$$

with $z_1(t)$ changing over time as more and more content gets released.

At time t_2 the DCV with its remaining content in the distal region from the supported membrane collapses into the SLB and diffuses together with the already released content laterally within the

cleft with an effective diffusion coefficient D_2 . It is possible that parts of the luminal matrix in which the NPY is embedded (18) is still intact and that the observed fluorescent decay is limited by a release step from this structure. The effective diffusion coefficient therefore describes both, the release from the matrix and the actual lateral diffusion away from the fusion site.

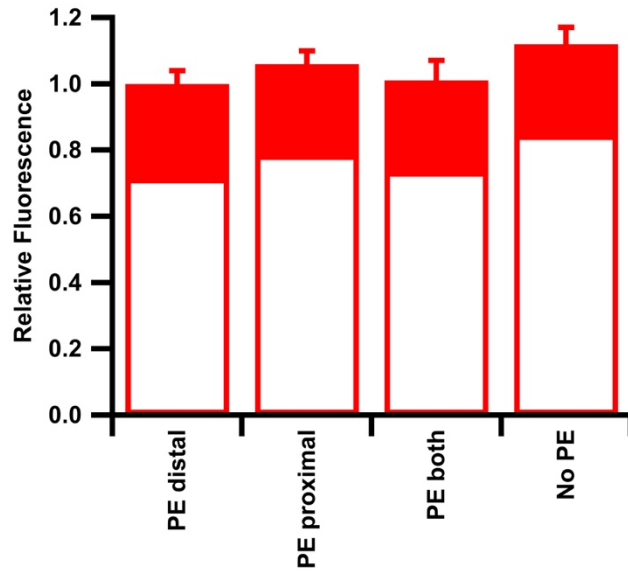
$$C_{LEFT}(t = t_2) = C_{LEFT}(x, y, z, t_2) + C_{DCV}(x, y, z, t_2) \quad (7)$$

$$dC_{LEFT}(t > t_2) = D_2 \Delta C_{LEFT} dt \quad (8)$$

At this time (t_2) we assume the remaining content to collapse into a plane corresponding to the surface area of the original DCV instantaneously. The total observable intensity which now originates only from the cleft becomes:

$$I_{LEFT}(t > t_2) = PSF(\lambda) * C_{LEFT}(x, y, z, t) e^{\frac{-z_{LEFT}}{d_p}} \quad (9)$$

We simulated the fluorescence intensity of the central pixel centered on a DCV using the above parameters and adjusting the length of the time period t_2-t_1 , the release rate k_r . The diffusion coefficients D_1 and D_2 were left unchanged from our previous results (14). Figure 1B shows the best simulated curves together with data for the four lipid conditions used. In the Supplemental Figure S1 we show each data set combined with the best fit simulation for all membrane conditions to illustrate the detected differences in fusion pore life times and release rates. In the shown simulations, the released DCV content diffuses away from the fusion site with a rate of $D_1 = 5 \mu\text{m}^2/\text{s}$ during pore opening and with a diffusion coefficient of $D_2 = 0.05 \mu\text{m}^2/\text{s}$ after collapse of the vesicle into the supported membrane. Both diffusion coefficients are significantly smaller than the reported diffusion coefficient for green fluorescent protein in solution ($D \approx 80 \mu\text{m}^2/\text{s}$, (31)) indicating that the content indeed diffuses in the cleft between the supported membrane and substrate where the molecular mobility is known to be impaired (32,33). The slower diffusion observed after the collapse of the DCV might be due to the high density of (protein-) material at the fusion site and a possible release step of NPY.



Supplemental Figure S2: Relative fluorescence intensity of Alexa546-syntaxin-14C co-reconstituted with SNAP-25A into different types of planar supported bilayers. The protein was labeled and fluorescence was measured as described in Liang et al. 2013 (22). All intensities were normalized to condition 1 and the error bars represent the standard deviation of 8 images. The open bar area represents the amount of fluorescence that was quenched after 500 mM Co^{2+} was added to the sample indicating that 70-75% of all Alexa546-syntaxin-14C was oriented with its N-terminus facing away from the substrate.

Condition	Proximal Leaflet	Distal Leaflet	Number of Experiments	Percent Fusion	Number of Docking	Number of Fusion	k (s ⁻¹)	m
PE Distal	70:30 bPC:Chol	25:25:15:30:4:1 bPC:bPE:bPS:Chol:PI:PIP2	14	41 ± 0.9	823	340	0.44 ± 0.1	4.8 ± 0.2
No PE	70:30 bPC:Chol	50:15:30:4:1 bPC:bPS:Chol:PI:PIP2	5	33.2 ± 3.4	340	113	0.47 ± 0.04	7.8 ± 1.1
PE Proximal	45:25:30 bPC:bPE:Chol	50:15:30:4:1 bPC:bPS:Chol:PI:PIP2	5	14.6 ± 1.7	419	58	0.38 ± 0.06	4.5 ± 1.0
PE Both	45:25:30 bPC:bPE:Chol	25:25:15:30:4:1 bPC:bPE:bPS:Chol:PI:PIP2	5	29.0 ± 3.1	455	134	0.38 ± 0.03	4.3 ± 0.5

Supplemental Table S1: Summary of statistics of DCV fusion events with planar supported bilayers under different PE lipid conditions. All events were fit with a parallel reaction model ($N(t) = N(1 - e^{-kt})^m$ where N is the fusion probability, k is the rate, and m is the number of parallel reactions occurring, see ref. 19) for the cumulative distribution function of delay times between docking and fusion for single DCV events under different PE lipid conditions. Errors for k and m represent standard fitting errors obtained from a nonlinear Levenberg-Marquardt fit algorithm (34).